Dynamics of Laser-Driven Shock Waves in Fused Silica

A. Ng, P. Celliers, and D. Parfeniuk
Physics Department, University of British Columbia, Vancouver, British Columbia, Canada V6T 2A6
(Received 12 August 1986)

The formation of laser-driven shocks in fused silica was observed from shock-trajectory measurements. The result reveals an anomalously slow buildup of the strong shock which suggests a significant volume change at pressures $\gtrsim 1$ Mbar. Nonsteady propagation of the strong shock was also observed for a transient period immediately following its formation.

PACS numbers: 47.40.Nm, 52.35.Tc, 62.50.+p

In recent years, the use of high-power lasers to drive strong shocks in solids has become a useful tool in high-pressure research.[1] Most of these experiments focused on the shock when it has steepened into a steady wave. The early stages of shock formation have not been studied in detail. During the rise of the laser pulse, the shock accelerates from the acoustic speed to its asymptotic value on the order of the pulse rise time. The thermodynamic state of the material behind the accelerating shock does not lie on the Hugoniot, but spans a region from the principal isentrope to the principal Hugoniot. As the ablation pressure must be transmitted through this region to reach the shock front, a detailed measurement of the shock trajectory will provide information about the isentrope as well as the Hugoniot.

Here we report on measurements of the trajectories of laser-driven shocks in fused silica. A double-wave structure was observed characteristic of the material,[2-5] and the asymptotic wave speed showed good agreement with the principal Hugoniot. However, the formation of the strong shock was anomalously slow for pressures exceeding 1 Mbar, and a transient nonsteady propagation of the strong shock was observed immediately following its formation.

In the experiment, fused-silica targets (2.2 g/cm^3) were irradiated with a 0.53-μm, $\sim$2-ns (FWHM) laser pulse from a Nd-glass laser. The laser beam was focused onto the 1-mm edge of the silica slab (1 mm$\times$2.5 cm$\times$7.5 cm) with $f/10$ optics at normal incidence. The intensity distribution at focus was nearly Gaussian with 60% of the laser energy contained in a spot of 45 to 100 μm diameter (average irradiance Φ_{60}) and 90% energy in a 75–170-μm-diameter spot (average irradiance Φ_{90}). The shock trajectory inside the target was measured with the use of streak shadowgraphy. A 0.57-μm dye-laser probe beam illuminated the target in a direction perpendicular to the 0.53-μm beam. The transmitted probe light was imaged onto the entrance slit of a streak camera (Hamamatsu C1370) such that the shock propagation was along the slit direction. To prevent the refraction of the probe light by the target corners from obscuring its front surface, the surface was polished to a small concave curvature. The optics viewed the first 100 μm of the target with ≤ 3 μm resolution. The target front surface was measured with ± 3 μm accuracy. By simultaneous display of a 0.53-μm laser fiducial on the camera, timing reference was measured to ± 100 ps accuracy. The laser pulse was also recorded with the use of a photodiode. Some schlieren measurements were also made.

Figure 1(a) shows a typical streak shadowgram. The dark region indicates transmitted probe light, whereas the bright region indicates that the probe light has either been absorbed in the target or refracted out of the collection optics. At low shock strengths, the interpretation of the boundary separating the dark and the bright regions is complicated by the fact that fused silica remains transparent at least up to the Hugoniot elastic limit of 100 kbar.[2] Furthermore, for pressures ≤ 35 kbar, a density-ramp precursor is known to propagate because of an anomalous increase in the compressibility of the material.[2,4] Thus at early times when the shock is weak, the leading front may not be visible in the shadowgram because of the relatively weak density discontinuity. Only when the shock becomes sufficiently strong, and the material sufficiently compressed and ionized, does the opaque boundary in the shadowgram yield an accurate detection of the shock front, as evident from Figs. 1(a) and 1(b). The sharp boundary observed in Fig. 1(a) at very early times is not clearly defined in the schlieren picture. It appears that this was not coincident with the shock front since the schlieren measurement revealed disturbances at a greater depth [Fig. 1(b)]. Such disturbances could be attributed to the low-pressure elastic wave. There may also be weak ionization due to early transmission of the 0.53-μm laser radiation before the formation of a plasma on the target surface. At later times, both the shadowgraphy and schlieren measurements are in clear agreement, yielding an accurate determination of the pressure front.

For laser irradiance (Φ_{60}) exceeding 10^{12} W/cm^2, all measurements, either shadowgraphy or schlieren, showed a characteristic double-wave structure [e.g., Figs. 1(a) and 1(b)]. The kink in the trajectory indicated a coalescence of a high-pressure wave with the initial low-pressure wave to form a single strong shock propagating

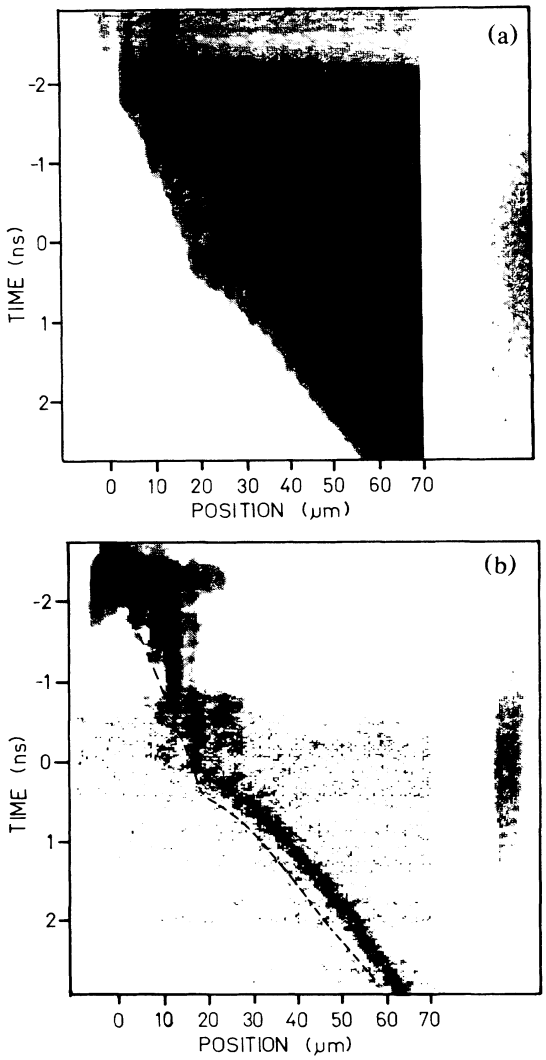

FIG. 1. x-t streak records: (a) shadowgram and (b) schlieren image. The dashed line in (b) corresponds to the optical boundary in (a).

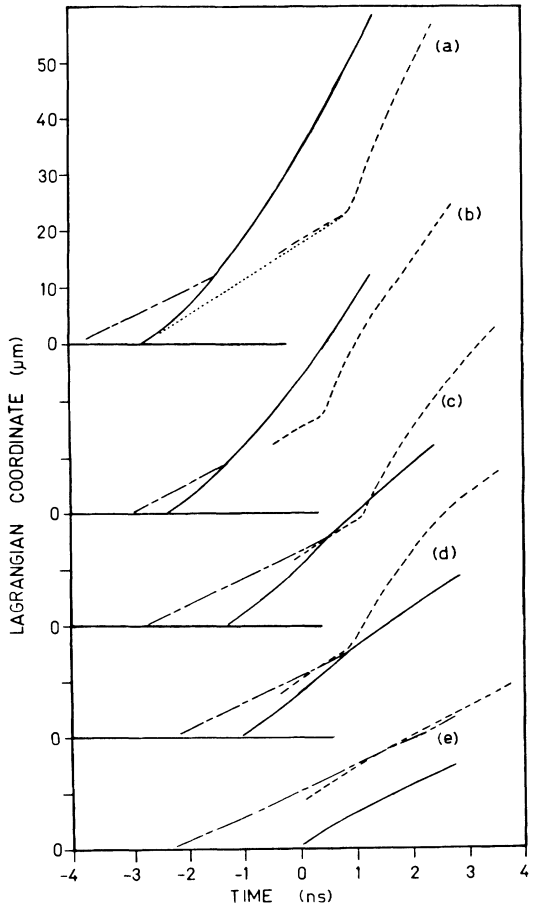

FIG. 2. Simulated trajectories: dot-dashed line represents the elastic precursor ($\rho = 2.3$ g/cm^3); solid line represents the high-pressure (stishovite) phase ($\rho = 4.0$ g/cm^3). Measured trajectories: dashed lines. The dotted line in (a) is for estimating $\langle D \rangle$. The experimental conditions for the five measurements (a)–(e) are laser pulse length (FWHM)=2.2, 2.0, 2.1, 2.1, 1.8 ns; absorbed irradiance $\Phi_{60} = 3\times10^{13}$, 1.5×10^{13}, 4×10^{12}, 2×10^{12}, 7×10^{11} W/cm^2; peak pressure = 5.5, 3.2, 1.6, 1.0, 0.56 Mbar.

at a much higher speed. Prior to the coalescence, the higher-pressure wave propagating behind the low-pressure wave could not be seen because of the opacity of the already compressed material. Another prominent feature of the observed trajectories is that the speed of the shock front reached transiently a peak value at the coalescence, but rapidly decreased to a steady, lower value.

Further interpretation of the data was made with the use of one-dimensional hydrodynamic simulations based on MEDUSA[6] with inverse bremsstrahlung absorption, Spitzer thermal conduction, and SESAME[7] equation of state. For the short-wavelength laser light and the modest irradiance used here, these should accurately model the laser absorption and ablation process[8] which generated the shock. The exact laser pulse shape as recorded by the photodiode (with dynamic range > 100) was used in the simulation.[9]

Figure 2 shows the results of the simulations for different laser irradiances. The stishovite transition of silica[3,10] is included in the SESAME equation of state. Thus, the calculations all reveal a double-wave structure indicative of a phase transition. By examination of the density and pressure profiles at various times in the simulations, it is easily seen that an elastic wave is launched at low pressures. When the elastic limit is exceeded at 100 kbar, the stishovite transformation starts to take place and a second wave develops which propagates more slowly than the elastic wave. This second wave begins to catch the elastic wave when the driving pressure exceeds

~300 kbar. The position and time of the coalescence of the high-pressure wave with the elastic wave depends on the laser irradiance. For a higher irradiance, coalescence occurs earlier. Following this the wave propagates as a single strong shock which will accelerate if the driving pressure continues to increase. During the process of shock formation, the material up to a depth of ~10 μm inside the target is never compressed by a strong shock. A strong shock is not formed until the various waves have steepened at greater depths in the target.

Also presented in Fig. 2 are the measured shock trajectories. The accuracy in the location of the measured trajectory is ± 3 μm and ± 100 ps. At sufficiently low irradiance [Fig. 2(e)] the experiment showed excellent agreement with the simulation. For all irradiances, the measured asymptotic shock speed was also in good agreement with that predicted by the simulations. At these late times the shock is located on the principal Hugoniot, as indicated in Fig. 3.

On the other hand, reasonable agreement between the measured and the calculated coalescence points was found only when the peak driving pressure was less than 1 Mbar. At higher peak pressures, the measured coalescence point occurred later and deeper in the target than predicted. In the worst case the discrepancy was 2.5 ns and 10 μm. This indicated that before the coalescence, the speed of the high-pressure wave was significantly lower than that predicted in the simulation. Although the propagation of this wave behind the elastic precursor could not be measured directly, its average speed $\langle D \rangle$ was estimated from the slope D' of the straight line [dotted line in Fig. 2(a)] connecting the calculated point of initial formation of the stishovite compression (the second wave) to the measured coalescence point as illustrated in Fig. 2(a). For the Lagrangian coordinate system used, $\langle D \rangle = D'\rho_i/\rho_e$, where $\rho_i = 2.2$ g/cm^3 is the initial target density and $\rho_e = 2.6$ g/cm^3 is the density behind the elastic precursor. The corresponding average $\langle p \rangle$ was estimated from the simulation by

$$\langle P \rangle = (t_2 - t_1)^{-1} \int_{t_1}^{t_2} P_A(t')dt',$$

where P_A is the pressure at the ablation front, t_1 the time of formation of the second wave, and t_2 the observed coalescence time. As shown in Fig. 3, for pressures > 1 Mbar the values of $\langle D \rangle$ are much lower than that given by the Hugoniot centered on the state behind the elastic wave. This suggests that a significant volume change occurs at ~1 Mbar since the speed of the high-pressure wave is given by $(1/\rho_0)\,|\Delta P/\Delta V|^{1/2}$.

A large volume collapse on the stishovite isentrope at ~1.25 Mbar has been reported by Pavlovskii *et al.*[11] and attributed to metallization of silica.[12,13] At these pressures the Hugoniots for fused or crystalline silica are far from the principal isentrope, and such transition has not been observed in other dynamic compression experiments.[14] As noted above, for the laser-driven shock, the material near the target surface is compressed nearly isentropically. It may therefore attain states close to those reached by Pavlovskii *et al.* The reported volume collapse would also be consistent with the present observation. However, there are strong arguments against such a phase transition in silica. The observed density[11] is in considerable disagreement with that calculated for the liquid phase.[15] Furthermore, no metallization was observed in static compression up to 2 Mbar,[16] although it may be argued that the temperature of the compressed material would be much lower than that obtained under isentropic compression.

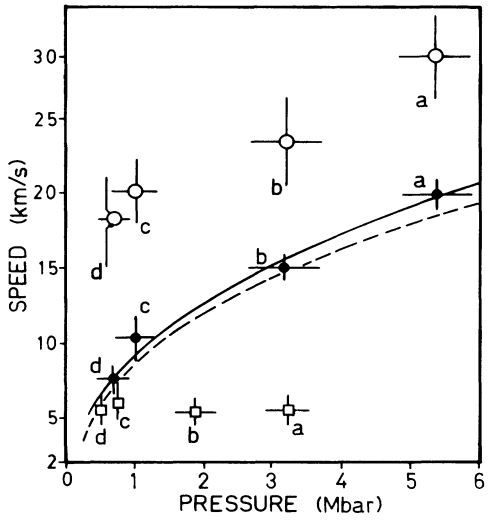

FIG. 3. Wave speed as a function of pressure. Solid circles, asymptotic speed; open circles, peak transient speed; open squares, average propagation speed behind the elastic precursor wave. Solid line, principal Hugoniot; dashed line, Hugoniot centered on the state behind the elastic wave.

Other processes not included in the SESAME data may also be considered. Shock melting of stishovite was observed[17] at ~1 Mbar. However, it yielded a negligible volume change. A multiphase equation of state including the chemical dissociation of silica has been calculated[18] up to a density of ~2.2 g/cm^3 and a corresponding pressure of ~100 kbar. Even at such a low density, significant dissociation results only at a relatively high temperature of 1 eV. For the high-density stishovite state with a temperature of < 0.5 eV of interest here, it is not clear if chemical dissociation would dominate. It was suggested[19] that a large volume collapse may result from the transformation of stishovite to a heterogeneous mixture of oxygen and liquid metal silicon.

As noted earlier, the observed speed of the single strong shock reaches a peak transient value immediately following the coalescence of the high-pressure wave with the elastic precursor. This transient speed lies much above the principal Hugoniot (Fig. 3). It then relaxes to

the Hugoniot value in a time scale of ~ 1 ns and a distance of $\sim 10\ \mu$m. In view of the transformation process conjectured, it is not surprising that the wave propagation following the coalescence is not steady. The transient may be due to a finite equilibration rate for the transformation process occurring behind the shock front. This effect is not seen in the simulations since a multiphase, nonequilibrium thermodynamic description would be required.

In conclusion, the formation of laser-driven shocks in fused silica has been examined from measurements of shock trajectories and from one-dimensional hydrodynamic simulations. The results revealed anomalously slow propagation of a high-pressure wave through the nearly isentropically compressed material. A high-speed transient was also observed which might provide information on the relaxation rate of the nonequilibrium state produced. It may also be noted that when the shock wave becomes steady, the shock speed (and hence the shock pressure) is in good agreement with predictions of the simulations. This implies that the transient processes occurring during shock formation should not cause degradation in the implosion of laser-fusion targets. The delay in the coalescence of the high-pressure and the elastic waves may affect the timing of the converging shocks depending on target design.

Invaluable discussions with N. W. Ashcroft and J. W. Shaner are gratefully acknowledged. We also wish to thank the Los Alamos National Laboratory for providing the SESAME data.

[1]F. Cottet, J. P. Romain, R. Fabbro, and B. Faral, Phys. Rev. Lett. **52**, 1884 (1984), and references therein.

[2]J. Wackerle, J. Appl. Phys. **33**, 922 (1962).

[3]R. G. McQueen, J. N. Fritz, and S. P. Marsh, J. Geophys. Res. **68**, 2319 (1963).

[4]L. M. Barker and R. E. Hollenbach, J. Appl. Phys. **41**, 4208 (1970).

[5]R. F. Trunin, G. V. Simakov, and M. A. Podurets, Phys. Solid Earth **2**, 102 (1971).

[6]J. P. Christiansen, D. E. T. F. Ashby, and K. V. Roberts, Comput. Phys. Commun. 7, 271 (1974).

[7]Table number 7380, SESAME Data Library, Los Alamos National Laboratory.

[8]D. Pasini, Ph.D. thesis, University of British Columbia, 1984 (unpublished).

[9]Details of the laser intensity as a function of time are available in tabular form upon request.

[10]S. M. Stishov and S. V. Popova, Geokhimiya **10**, 837 (1961).

[11]A. I. Pavlovskii, N. P. Kolokol'chikov, M. I. Dolotenko, and A. I. Bykov, JETP Lett. **27**, 264 (1978) [Pis'ma Zh. Eksp. Teor. Fiz. **27**, 283 (1978)].

[12]L. F. Vershchagin, E. N. Yakovlev, B. V. Vinogradov, V. P. Sakun, and G. N. Stepanova, JETP Lett. **20**, 215 (1974) [Pis'ma Zh. Eksp. Teor. Fiz. **20**, 472 (1974)].

[13]N. Kawai and A. Nishiyama, Proc. Jpn. Acad. **50**, 72 (1974).

[14]J. N. Fritz, and R. G. McQueen, in *Shock Waves in Condensed Matter,* edited by J. R. Asay, R. A. Graham, and G. K. Straub (Elsevier, Amsterdam, 1984), p. 73.

[15]A. E. Carlsson, N. W. Ashcroft, and A. R. Williams, Geophys. Res. Lett. **11**, 617 (1984).

[16]H. K. Mao, private communication.

[17]G. A. Lyzenga and T. J. Ahrens, J. Geophys. Res. **88**, 2431 (1983).

[18]F. H. Ree, Lawrence Livermore Laboratory Report No. UCRL-52153, 1976 (unpublished).

[19]N. W. Ashcroft, private communication.